Title: Loss-of-function mutations in *ASIP* and *MC1R* are associated with coat colour variation in marsupials.

Authors

Ryan Sauermann[1], Bronwyn Fancourt[2,3], Tim Faulkner[4], Hayley Shute[4], Dean Reid[4], Andrew J. Pask[1,5], Charles Y. Feigin[1,6*]

Affiliations

1. School of BioSciences, The University of Melbourne, VIC, Australia.
2. School of Environmental and Rural Science, University of New England, Armidale, NSW, Australia.
3. Queensland Parks & Wildlife Service, Department of the Environment, Tourism, Science & Innovation, Toowoomba, QLD, Australia.
4. Australian Reptile Park & Aussie Ark, Somersby, NSW, Australia.
5. Department of Sciences, Museums Victoria, Carlton, VIC Australia.
6. Department of Ecological, Plant and Animal Sciences, La Trobe University, Bundoora, VIC, Australia.

*Correspondence: c.feigin@latrobe.edu.au

Abstract

Pigment production in mammalian hair follicles is governed in part by interactions between Agouti Signalling Protein (ASIP) and the Melanocortin 1 Receptor (MC1R). The most common coat colours in mammals result from alternating bands of dark eumelanin and light pheomelanin within individual hairs. However, coats dominated by a single type of melanin have arisen several times. Here, we examine the genetic basis of two instances among the marsupials: a melanistic morph of the eastern quoll (*Dasyurus viverrinus*) found at high frequency in the wild, and a rare case of fixed xanthism in the marsupial moles. In the eastern quoll, we show that a deletion

encompassing part of the *ASIP* coding sequence likely explains melanism in this species. Notably, this mutation is convergent with that recently discovered in its dark-coated relative, the Tasmanian devil (*Sarcophilus harrisii*). Conversely, we show that a nonsense mutation which severely truncates *MC1R* in the southern marsupial mole (*Notoryctes typhlops*) is a strong candidate driver of its pheomelanin-predominant coat. Together with other recent findings, our results suggest that loss-of-function mutations have occurred repeatedly within the marsupials, representing an important mechanism underpinning coat colour variation.

Introduction

Coat colour in mammals results from the quantities and spatial distributions of two types of pigment, dark eumelanin and light pheomelanin[1]. Within the hair follicle, these pigments are regulated in part by secretion of Agouti Signalling Protein (ASIP) from dermal papilla (DP) cells, which acts in a paracrine manner on pigment-producing melanocytes by binding to the Melanocortin 1 Receptor (MC1R)[2]. MC1R constitutively promotes the production of dark eumelanin, a function that is enhanced by its agonist, α-MSH. ASIP functions as an inverse agonist, both competing with α-MSH to bind MC1R and reducing MC1R's activity, leading to a shift toward production of light pheomelanin[2]. The most common dorsal coat colours in mammals, ranging from grey to light brown, result from alternating bands of pheomelanin and eumelanin within individual hair shafts, a phenotype called agouti (figure 1a-c)[1]. By contrast, patterns that span many follicles, including stripes and spots, are regulated by mechanisms that establish spatial information across whole skin regions, such as reaction-diffusion systems and long-range morphogens[3].

Loss of a single type of melanin can arise through mutations that modify or inhibit regulators of pigment production. Among the most common examples in mammals is melanism, a phenotype in which eumelanin is produced exclusively or in elevated quantities, leading to dark brown or black hair. Genetic studies have linked several cases of melanism with either loss-of-function (LoF) mutations in *ASIP*, or gain-of-function (GoF) mutations in *MC1R*[4-6]. Conversely, coat phenotypes arising from overproduction of pheomelanin appear to be rarer, or more poorly documented in wild mammals[7, 8]. Such phenotypes can be classified as xanthism or xanthochromism when pheomelanin is yellow in colour, or erythrism when it has a more orange to red hue[9]. Better documented are cases of leucism and albinism, which involve loss of pigmentation. While often considered chromatic disorders[8], these phenotypes are not intrinsically deleterious and their fitness consequences depend on ecological context.

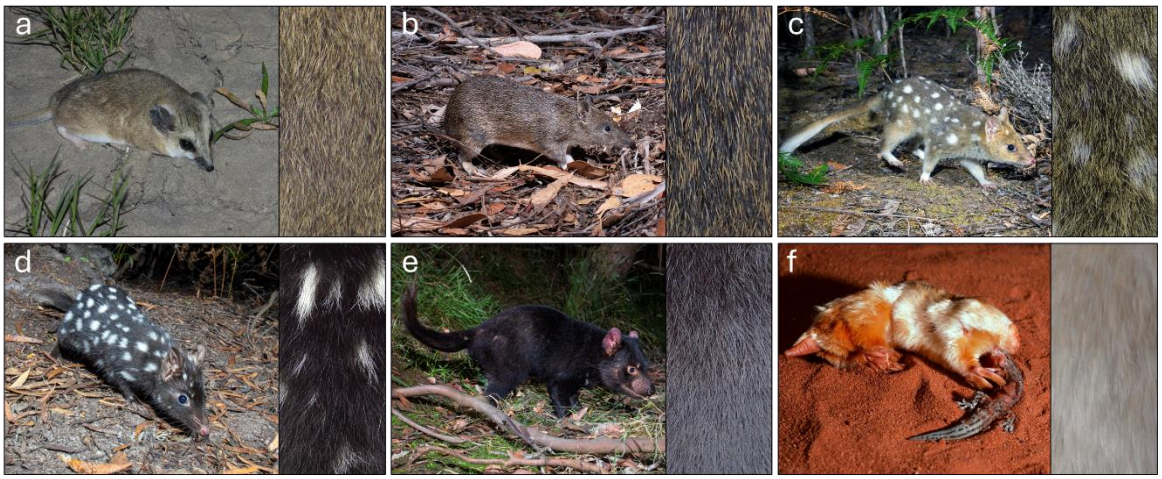

Figure 1: Illustration of marsupial coat colour variation. Species such as the fat-tailed dunnart (*Sminthopsis crassicaudata*; a) and southern brown bandicoot (*Isoodon obesulus*; b) exhibit the typical mammalian agouti pattern with alternating bands of pheomelanin and eumelanin. The eastern quoll (*Dasyurus viverrinus*) has two common colour morphs, a wildtype "fawn" morph (c) with an agouti background coat and a melanistic "black" morph (d). The Tasmanian devil (*Sarcophilus harrisii*; e) a solid black background coat. The marsupial moles (illustrated here by the southern species, *Notoryctes typhlops*; f) typically have a pale-yellow coat. Credits for animal photographs: Lachlan Copeland (a), Brett Vercoe (b-e), Mike Gillam (f).

Coats dominated by one type of melanin have arisen multiple times in marsupials, including instances where they have become fixed in a species (figure 1d-f). For example, we recently showed that in the Tasmanian devil (*Sarcophilus harrisii*), a LoF mutation in *ASIP* likely contributes to the species' distinctive, black coat (figure 1e)[10]. Interestingly, a similar phenotype exists as a high frequency polymorphism in the closely related and parapatric eastern quoll (*Dasyurus viverrinus*; figure 1c,d)[11]. Additionally, the marsupial moles (Genus *Notoryctes*), which comprise two cryptic, fossorial species native to Australia's great deserts, exhibit a cream to pale yellow colour (figure 1f)[12]. This phenotype represents a rare case of fixed xanthic coloration in a wild mammal.

Here, we examine the genomic basis of coat colour in the eastern quoll and southern marsupial mole. First, using a new haplotype-phased assembly of the eastern quoll and resequencing of phenotyped individuals, we show that a deletion at the *ASIP* locus likely underpins its melanistic morph. Interestingly, this mutation is convergent with that found the closely related Tasmanian devil[10]. Further, by examining the *MC1R* locus across agreodont marsupials (comprising the orders light-yellow, Peramelemorphia and Notoryctemorphia)[13, 14] we identify a nonsense mutation that severely truncates the receptor as a candidate for the marsupial mole's distinctive light yellow coat. Our results align with several recent findings in other marsupials, illustrating that LoF changes in core pigment regulating genes are potentially important mechanisms for the evolution of coat colour in this lineage.

Results

Haplotype-phasing identifies a deletion at the eastern quoll *ASIP* locus

We recently generated a reference genome for the eastern quoll (DasViv_v1.0)[10]. This animal exhibited the wildtype "fawn" colour morph, which is characterized by

87 agouti banded background fur, punctuated by white (pigment-free) spots (figure 1c).
88 A melanistic morph, which exhibits black background fur while retaining white spots
89 (figure 1d), is also found at high frequency in both wild and captive populations,
90 occurring at a ratio of approximately 1:3 relative to the fawn morph[15-17]. This has
91 lead to the hypothesis that melanism in eastern quolls has a recessive pattern of
92 inheritance[17]. Given that *ASIP* LoF is a driver of melanism in other mammals and
93 is expected to be recessive based on its molecular function, we first asked whether
94 our fawn-coloured reference individual may have been a carrier for such a mutation.
95 To this end, we generated a new, haplotype-phased genome of the eastern quoll by
96 reassembling PacBio HiFi and Omni-C reads that were used to produce the previous
97 pseudohaplotype genome. The two resulting haplotypes were named
98 DasViv_v2.0_hap1 and DasViv_v2.0_hap2 (hereafter, referred to as haplotype 1 and
99 haplotype 2, respectively). Scaffold metrics for each haplotype were comparable to
100 those of DasViv1.0 (table S1).

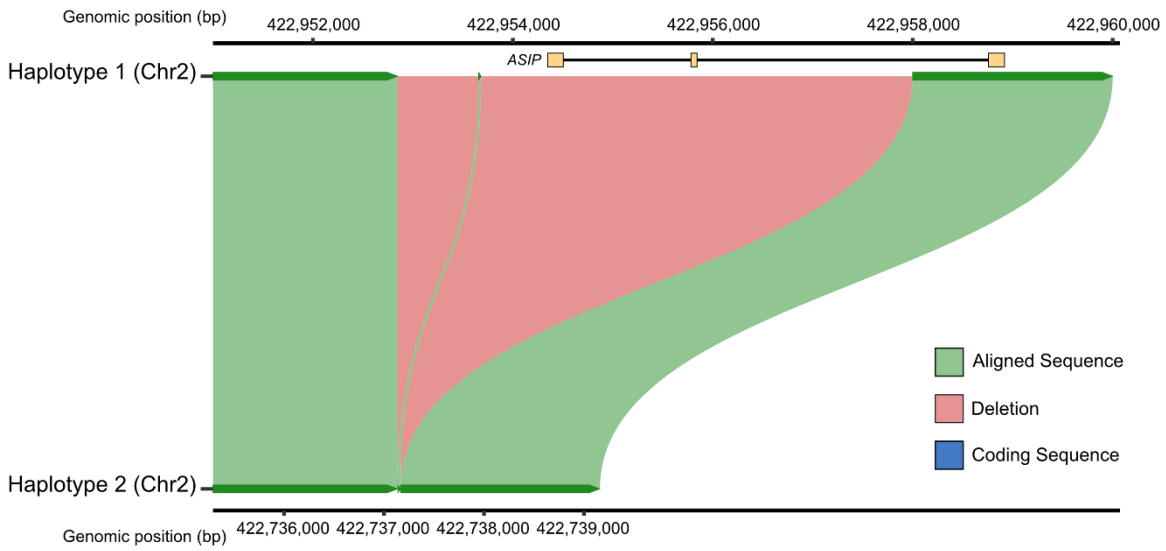

Figure 2: Alignment of the eastern quoll *ASIP* locus, centred on the deletion region. Green ribbons represent sequences aligned between haplotype 1 (top) and haplotype 2 (bottom). Red ribbons represent the putative deletion region, which is present in haplotype 1 but absent from haplotype 2. Coding exons (i.e. CDS annotations) for *ASIP* are shown in yellow above the alignment, illustrating that the first two coding exons are deleted.

101 To facilitate examination of the *ASIP* locus, we next annotated this gene in each
102 eastern quoll haplotype assembly, as well as assemblies of several related
103 marsupials (table S2). Interestingly, while the *ASIP* allele annotated on haplotype 1
104 contained a complete coding sequence as in other marsupials with typical agouti
105 banded hair, annotation of the first two coding exons on haplotype 2, including the
106 start codon, was unsuccessful (data S1). Blastn searches for these exons similarly
107 returned no hits against haplotype 2[18]. Given this, we next extracted the genomic
108 region surrounding the expected locations of these exons from both eastern quoll
109 haplotypes. Alignment of these sequences revealed a ~4.7 kb stretch of sequence
110 missing in eastern quoll haplotype 2 and encompassing the first two coding exons
111 (figure 2, data S2). This observation indicated that the individual used to generate
112 the eastern quoll reference genome was indeed heterozygous for a presumptive LoF
113 mutation at the *ASIP* locus. This, together with the animal's fawn colour, is also
114 consistent with melanism having a recessive pattern of inheritance. Interestingly, the
115 eastern quoll *ASIP* deletion appears to be convergent with the fixed *ASIP* deletion
116 recently identified in a closely related dasyurid marsupial, the Tasmanian devil. Both
117 deletions share an extremely similar 5' break point, though the devil mutation only
118 encompasses the first coding exon (data S2)[10].

119 <u>Resequencing supports recessive melanism caused by *ASIP* deletion</u>

120 To further explore this finding, we sequenced genomic DNA from fawn (n = 3) and
121 black morph (n = 3) eastern quolls and visualized mapping coverage against eastern
122 quoll haplotype 1 (which retains the intact *ASIP* locus). This revealed that all black
123 morph quolls showed zero mapping coverage over the genomic interval that
124 corresponded to the *ASIP* deletion on eastern quoll haplotype 2, while all fawn
125 morph quolls showed high coverage (figure 3). This indicated that all black morph

126 quolls are homozygous for this deletion, reinforcing that a recessive LoF mutation

127 likely explains melanism in eastern quolls.

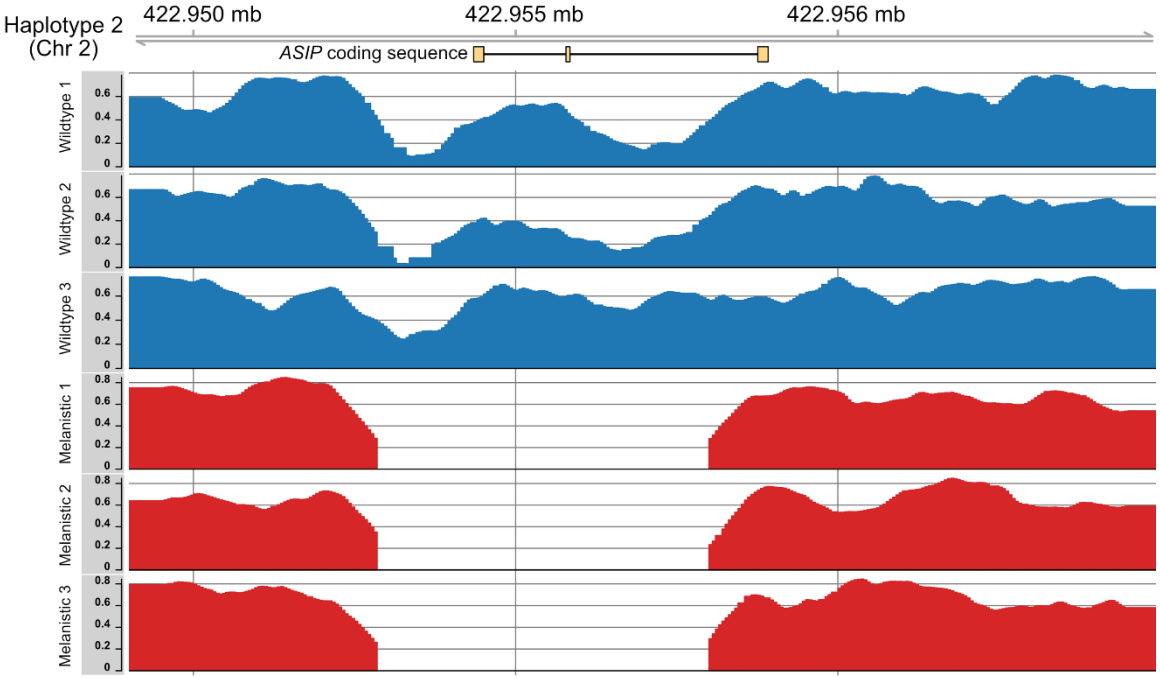

Figure 3: Read mapping coverage of wildtype and melanistic eastern quolls across the *ASIP* locus. Melanistic quolls (red) show no read coverage across the 4.7kb deletion region, indicating homozygosity for this mutation whereas all wildtype quolls exhibit high coverage.

128 <u>Truncation of MC1R likely drives yellow coat colour in marsupial moles</u>

129 Another notable instance among agreodonts where agouti banding has been lost is

130 in the marsupial moles. Comprising two species, the northern and southern

131 marsupial moles (*Notoryctes caurinus* and *Notoryctes typhlops*, respectively), this

132 desert-dwelling group has evolved a suite of convergent adaptations with eutherian

133 moles to facilitate its fossorial lifestyle, including highly reduced eyes and modified

134 forelimbs which they use to “swim” through loose sands[13, 19]. They are among the

135 most rarely observed mammals in Australia, with only a handful of reported sightings

136 each decade. All documented individuals have been found to exhibit a cream to pale

137 yellow pelage, with no obvious sign of dark eumelanin deposition (figure 1f)[20]. We

138 recently generated a reference genome for the southern marsupial mole and thus

139 sought to explore the basis of this species' unique coat colour[13]. Given the

140 constitutive function of MC1R in eumelanin production, we hypothesized that a LoF

141 at this locus might contribute to its apparent absence in marsupial mole hair.

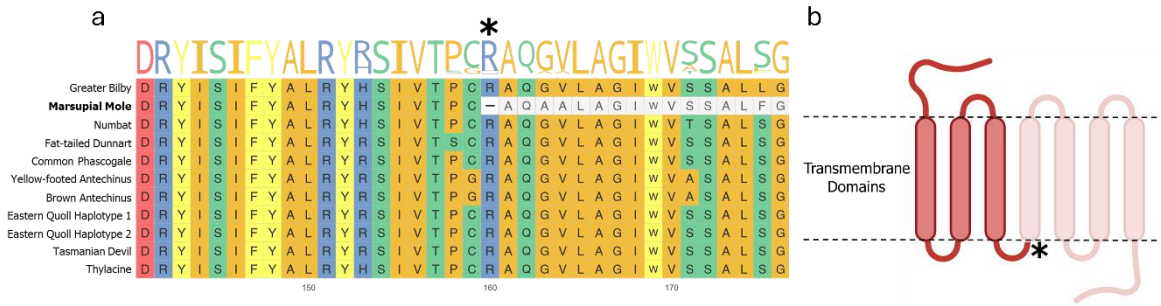

Figure 4: (a) Partial view of aligned amino acid sequences of MC1R orthologs across examined marsupials. Colours indicate residues with similar side chain properties. The sequence logo represents the frequency of different residues at each position. The asterisk indicates the location of the identified nonsense mutation in the marsupial mole, with the truncated bases shown in grey. (b) A diagram of the MC1R protein showing domains ablated by this change.

142 As *MC1R* was successfully annotated in all marsupial genomes tested, we translated

143 and aligned the amino acid sequences of its orthologs. Interestingly, we found that

144 while *MC1R* was overall highly conserved across these species, a single gap was

145 present, exclusively in the marsupial mole. Examination of the nucleotide alignment

146 at this position showed that the gap was due to an in-frame stop codon at position

147 160, in place of a highly conserved arginine residue (R160X; figure 4a, data S3).

148 Based on the UniProt structural annotation of mouse MC1R (A0A0B6VTJ4),

149 truncation from the homologous residue (R158 in mouse) is expected to ablate ~50%

150 of the protein's length, including 4 of 7 transmembrane domains (figure 4b)[21, 22].

151 **Discussion**

152 Here, we provide evidence that repeated loss-of-function mutations in core pigment

153 regulating genes have contributed to coat colour variation within and between

154 marsupial species. We showed that in eastern quolls, a deletion in the *ASIP* locus is

155 associated with the common melanistic morph. Ablation of the only annotated start

156 codon and two complete coding exons likely prevents translation of a functional

protein product, resulting in a complete loss of ASIP's function as an inverse agonist of MC1R. *ASIP* LoF mutations have previously been associated with melanism in various other mammals[4-6]. Intriguingly, this mutation appears to be convergent with a similar deletion recently identified in its close relative, the Tasmanian devil (data S1 & 2)[10]. While differing in size (the devil deletion encompasses only the first coding exon), we expect the effects of these mutations to be similar, due to the loss of the start codon. Of note, the 5' breakpoints of the Tasmanian devil and eastern quoll deletions are very close in position (data S2). Sequence similarity between genomic regions flanking the deletion region on each haplotype, including several species-specific indels, strongly suggests that the eastern quoll mutation occurred independently from that in the Tasmanian devil. Thus, their deletions are likely convergent, rather than reflecting a shared ancestral variant. As the devil and quoll are closely related and dasyurid genome structure is highly conserved, sequence composition at this locus may have contributed to such similar, convergent deletions occurring in these sister genera[23].

Dark pelage has evolved in other marsupials, including brushtail possums (*Trichosurus vulpecula*), a phenotype recently shown to be driven by a mutation in the *ASIP* coding sequence[24]. The co-occurrence of multiple dark-coated species in Tasmania was noted by Bond et al. 2024, with several possible explanations explored[24]. One hypothesis proposed was a fitness benefit for darker fur colour in Tasmania's humid climates, in line with Gloger's rule[25]. Clear data on the frequency of fawn and black morph quolls across Tasmanian environments is not currently available. However, Tasmania as a whole became separated from mainland Australia around ~14,000 years ago at the end of the Last Glacial Maximum (LGM), and represents the Southern end of the species' historical range[26]. Black morph

eastern quolls were readily observed across Southeastern Australia prior to their extirpation from the mainland in the late 20th century[17, 27]. Presuming the genetic basis of melanism was shared between mainland and modern Tasmanian populations, it is likely that black morph eastern quolls persisted in quite diverse environments and through periods of climatic change. Thus, it remains unclear whether Gloger's rule provides a sufficient explanation for its relative abundance.

An alternative explanation proposed was crypsis, for example to avoid predation by the recently extinct Tasmanian tiger or thylacine (*Thylacinus cynocephalus*), reflecting an example of the "ghosts of predators past"[24, 28]. A similar hypothesis was recently proposed to explain the balanced frequencies of two colour morphs, green and olive, in the flightless Kākāpō parrot of New Zealand[29]. Unlike the Kākāpō colour polymorphism though, eastern quolls in Tasmania and the historic mainland populations show a roughly 3:1 ratio of fawn and black animals among both adults and pouch young, in line with mendelian expectations[17]. This does not rule out an advantage for dark fur and indeed it is quite notable that an extremely similar deletion at the *ASIP* locus has become fixed in the Tasmanian devil, potentially implying selection in favour of dark pelage. Both species may have been preyed upon by the thylacine, and as Bond et al. 2024 notes, the Tasmanian devil itself may continue to impose similar pressures on eastern quolls. Future population-scale studies of eastern quolls, including historical specimens prior to the extinction of the thylacine and the collapse of Tasmanian populations driven by devil facial tumour disease[30], may provide further insights.

In stark contrast to the eastern quoll and Tasmanian devil, marsupial moles appear to have lost eumelanin production in their fur altogether, a rare phenotype in mammals. Our analyses indicate that an early stop codon that truncates ASIP's

207 receptor, MC1R, is likely a contributing factor. Experiments using CRISPR-Cas9 to
208 truncate the rabbit ortholog of *MC1R* result in a light yellow coat, due to the loss of
209 eumelanin deposition into the hair shaft[31]. This strongly suggests that the natural
210 truncation of marsupial mole MC1R contributes to its distinctive coat colour. Rabbits
211 in which *MC1R* has been knocked out appear to exhibit a fairly striking yellow hue,
212 reminiscent of spontaneous xanthism/xanthochromism observed in various wild
213 mammals[7-9, 31], whereas the dorsal fur of marsupial moles is a paler yellow or
214 cream colour (figure 1f). This suggests that in addition to the loss of eumelanin
215 production, marsupial moles may also exhibit a degree of hypopigmentation.
216 Pseudogenization of *MC1R* has previously been linked to leucism in cave fish, but
217 not to our knowledge in mammals. Therefore, mutations at other loci involved in
218 pigmentation may contribute to the marsupial mole's overall coat colour[32]. Specific
219 regions of the marsupial mole's fur, such as the anterior aspect of the forelimbs and
220 posterior aspect of the hindlimbs, show prominent yellow coloration more typical of
221 xanthism in other species (figure 1f, figure S1). Colour variation across the marsupial
222 mole's coat may therefore reflect subtle developmental patterning. Notably, the
223 genus *Notoryctes* comprises two distinct species, the southern marsupial mole
224 (examined here) and northern marsupial mole, both of which share a similar coat
225 colour[20]. Molecular studies indicate that these sister species diverged around 4.6
226 million years ago[19], strongly suggesting that the loss of eumelanin production
227 through MC1R LoF may have arisen prior to their divergence.

228 Xanthism and leucism are rare in wild mammals, likely due to a fitness cost for
229 conspicuous coloration and are considered chromatic disorders[7, 33]. Thus, for
230 such a phenotype to be fixed in marsupial moles is remarkable. While these animals
231 are fossorial, their lighter coloration may provide some camouflage (depending on

232 the colour of local sands) or may contribute somewhat to thermoregulation when the
233 animal briefly emerges on the surface. While such periods may be short, predation
234 risk or sun exposure may provide some benefit to their coat colour.

235 Our results suggest that loss-of-function mutations in the pigment regulators *ASIP*
236 and *MC1R* contribute to coat colour in the eastern quoll and marsupial mole
237 respectively. Taken together with recent findings in related marsupials, they suggest
238 that loss-of-function mutations in core pigment regulation genes may represent an
239 important mechanism for the evolution of coat colour in this lineage. Our work further
240 invites new investigations into the potential adaptive implications of such mutations.

241 **Methods**

242 Genome Assembly

243 PacBio HiFi (~97.68 gigabases) and Omni-C (~126 gigabases) reads (NCBI
244 BioProject PRJNA75870) previously used to produce a pseudohaplotype assembly
245 of a female, fawn morph eastern quoll were reanalysed to produce a new haplotype-
246 phased assembly[10]. Briefly, PacBio reads were provided as input to hifiasm
247 v0.15.4-r343 with default parameters to produce primary scaffolds[34]. Next, Omni-C
248 reads were aligned against the assembly with bwa mem v0.7.17. The alignment and
249 assembly were then provided to the HiRise pipeline (Dovetail Genomics; Scotts
250 Valley, CA USA) yielding two haplotype assemblies[35]. Assembly quality for each
251 haplotype was compared to that of the original pseudohaplotype genome using
252 BUSCO v5.8.2 (parameters -m genome -l mammalia_odb10) and the stats.sh script
253 provided by the bbmap package with default parameters (table S1)[36, 37]. Scaffold
254 metrics and BUSCO gene recovery were roughly the same between the original
255 pseudohaplotype assembly (DasViv_v1.0) and each haplotype assembly
256 (DasViv_v2.0_hap1 and DasViv_v2.0_hap2, respectively) with marginal

257 improvements in ‘Complete Single Copy’ and ‘Missing’ ortholog categories when the
258 complete haplotype-phased assembly is taken together.

259 Identification and alignment of *ASIP* and *MC1R* orthologs

260 To identify orthologs of *ASIP* and *MC1R* across agreodont marsupials (table S2)[10,
261 30, 38-43], we used the program LiftOff v1.6.3[44] (default parameters) to perform
262 lift-over annotations. To avoid potential biases introduced by using a reference
263 species with divergent pigmentation, we used the high-quality RefSeq gene models
264 from the agouti-patterned yellow-footed antechinus (*Antechinus flavipes*)[38]. CDS
265 sequences of *ASIP* and *MC1R* were then extracted from each genome using Gffread
266 v0.9.12[45] and aligned using the MAFFT web server
267 (https://mafft.cbrc.jp/alignment/software/)[46]. Searches for *ASIP* coding regions
268 missing in eastern quoll haplotype 2 were performed using Blastn v2.16.0+[18]. As
269 no hits were returned, no results are shown. MC1R orthologs from all examined
270 marsupial genomes were translated and realigned with MAFFT. Visualization of the
271 MC1R amino acid alignment was performed using the R package ggmsa
272 v1.13.1[47].

273 Alignment and visualization of the *ASIP* genomic locus

274 Using the location of annotated *ASIP* exons identified by LiftOff, we extracted the
275 *ASIP* locus from both eastern quoll haplotypes as well as the Tasmanian devil, which
276 were aligned using the MAFFT web server as above. To produce the visualization
277 shown in figure 2, the *ASIP* locus in eastern quoll haplotypes 1 and 2 were realigned
278 with minimap2 v2.28-r1209 (parameters: -x asm20 --eqx --secondary=no -c) and
279 plotted using the R package SvbyEye v0.99.0[48, 49].

280 Eastern quoll resequencing

281 Tissue samples of six eastern quolls of known colour morph (n = 3 fawn, n = 3 black;
282 table S3) were acquired as secondary use from the Aussie Ark captive breeding
283 sanctuary (Somersby, NSW, AU) and through prior field collections on Bruny Island
284 under University of Tasmania Animal Ethics Committee Ethics Approval Permit
285 A11655 and Department of Primary Industries, Parks, Water and Environment
286 permits FA10042 and FA11050. DNA was extracted with the DNeasy Blood & Tissue
287 Kit (Qiagen, Cat. No. 69504). Libraries were prepared using the VAHTS Universal
288 Pro DNA Library Prep Kit for Illumina (Vazyme Cat. No. ND610) and were
289 sequenced to a depth of at least 25X coverage on an Illumina NovaSeq S4 flow cell
290 by Azenta Life Sciences (Burlington, MA, USA).

291 Raw reads were filtered for quality and residual adaptors using fastp (default
292 parameters) and then mapped against DasViv_v2.0_hap1, which retains a complete
293 copy of the *ASIP* locus, using bwa-mem2 v 2.2.1 (parameter -M)[50]. Alignments
294 were filtered using samtools view v1.13 to retain only primary alignments with a
295 MAPQ greater than 30 and properly paired reads (parameters -f 3 -F 3340 -q
296 30)[51]. Normalization for mapping coverage and conversion to bedgraph format
297 were performed using deepTools bamCoverage v3.5.5 (--scaleFactor 10 --
298 normalizeUsing BPM --exactScaling --normalizeUsing BPM)[52]. Visualization of
299 read coverage over the region shown in figure 3. was performed using the R
300 package Gviz v1.50.0[53].

301 **Data Availability**

302 Eastern quoll haplotype assemblies 1 and 2 are available on NCBI under BioProjects
303 PRJNA1209419 and PRJNA1209418, respectively. Whole genome resequencing
304 reads are available under BioProject PRJNA1209406. All original code used in this
305 study is attached as supplementary material in code S1-S3. The marsupial mole

photograph used in figure 1F is copyrighted (Mike Gillam/AUSCAPE, all rights reserved) and included here on a single use, non-exclusive license.

Contributions

C.Y.F. conceived the study and wrote the manuscript with editing by all co-authors. C.Y.F. and R.S. performed computational analyses. R.S. processed samples. B.F. provided subsamples of wild individuals. T.F. H.S. and D.R. provided subsamples of captive individuals. A.J.P. provided computational resourcing and sequencing support.

Acknowledgements

This study was supported by a Wild Genomes grant from Revive & Restore (Contract no. 2020-017) and through philanthropic support by the Wilson Family Trust. We thank Cantata Bio LLC for assistance producing the haplotype-phased eastern quoll genome, Rodrigo Hamede and Christopher Burridge of the University of Tasmania for help with sample logistics, Lachlan Copeland, Brett Vercoe and Mike Gillam for the use of marsupial photographs, Museums Victoria for permission to photograph pelts and Elise Ireland for extensive proofreading.

References

1. McRobie H.R., King L.M., Fanutti C., Symmons M.F., Coussons P.J. 2014 Agouti signalling protein is an inverse agonist to the wildtype and agonist to the melanic variant of the melanocortin-1 receptor in the grey squirrel (Sciurus carolinensis). *FEBS Letters* **588**(14), 2335-2343. (doi:10.1016/j.febslet.2014.05.032).
2. Suzuki I., Tada A., Ollmann M.M., Barsh G.S., Im S., Lamoreux M.L., Hearing V.J., Nordlund J.J., Abdel-Malek Z.A. 1997 Agouti signaling protein inhibits melanogenesis and the response of human melanocytes to alpha-melanotropin. *The Journal of investigative dermatology* **108**(6), 838-842. (doi:10.1111/1523-1747.ep12292572).
3. Johnson M.R., Li S., Guerrero-Juarez C.F., Miller P., Brack B.J., Mereby S.A., Moreno J.A., Feigin C.Y., Gaska J., Rivera-Perez J.A., et al. 2023 A multifunctional Wnt regulator underlies the evolution of rodent stripe patterns. *Nature ecology & evolution* **7**(12), 2143-2159. (doi:10.1038/s41559-023-02213-7).
4. Eizirik E., Yuhki N., Johnson W.E., Menotti-Raymond M., Hannah S.S., O'Brien S.J. 2003 Molecular genetics and evolution of melanism in the cat family. *Current biology : CB* **13**(5), 448-453. (doi:10.1016/s0960-9822(03)00128-3).

5. Kingsley E.P., Manceau M., Wiley C.D., Hoekstra H.E. 2009 Melanism in peromyscus is caused by independent mutations in agouti. *PLoS One* **4**(7), e6435. (doi:10.1371/journal.pone.0006435).
6. McRobie H.R., Moncrief N.D., Mundy N.I. 2019 Multiple origins of melanism in two species of North American tree squirrel (Sciurus). *BMC Evol Biol* **19**(1), 140. (doi:10.1186/s12862-019-1471-7).
7. Fuentes R., Castillo M., Moreno R., Quintero-Arrieta H., Pérez E., Araúz J., Añino Y., Murcia-Moreno D., Valdés R., Bonilla B., et al. 2024 Report of coloration anomalies in mammals from Panama. *Neotropical Biology and Conservation* **19**(3), 333-345. (doi:10.3897/neotropical.19.e125890).
8. Cotts L., Prestes S.B.S., Pires J.R., Mathias M.d.L. 2023 The first record of partial xanthochromism in big-eared opossum, Didelphis aurita (Didelphimorphia, Didelphidae). *Mammalia* **87**(6), 583-586. (doi:doi:10.1515/mammalia-2023-0104).
9. Cotts L., Costa G., Gabriel S.I., Rocha Barbosa O., Braga C. 2024 Unveiling the Colors of Mustelids: A Historical Review on the Emergence of Chromatic Disorders and Their Ecological Effects in Mustelids Worldwide with Report of the First Case of Erythrism in Eira barbara (Carnivora, Mustelidae). *Animals : an open access journal from MDPI* **14**(23). (doi:10.3390/ani14233354).
10. Hartley G.A., Frankenberg S.R., Robinson N.M., MacDonald A.J., Hamede R.K., Burridge C.P., Jones M.E., Faulkner T., Shute H., Rose K., et al. 2024 Genome of the endangered eastern quoll (Dasyurus viverrinus) reveals signatures of historical decline and pelage color evolution. *Communications Biology* **7**(1), 636. (doi:10.1038/s42003-024-06251-0).
11. Jones M.E., Rose R.K. 2001 Dasyurus viverrinus. *Mammalian Species* (677), 1-9. (doi:10.2307/0.677.1).
12. Ginsberg J.R. 2013 Mammals, Biodiversity of. In *Encyclopedia of Biodiversity (Second Edition)* (ed. Levin S.A.), pp. 681-707. Waltham, Academic Press.
13. Frankenberg S.R., Lucas S., Feigin C.Y., Doronina L., Steffen R., Hartley G., Grady P., Menzies B.R., De Paoli-Iseppi R., Donnellan S., et al. 2025 Unearthing the secrets of Australia's most enigmatic and cryptic mammal, the marsupial mole. *Science Advances* **11**(1), eado4140. (doi:doi:10.1126/sciadv.ado4140).
14. Beck R.M.D., Travouillon K.J., Aplin K.P., Godthelp H., Archer M. 2014 The Osteology and Systematics of the Enigmatic Australian Oligo-Miocene Metatherian Yalkaparidon (Yalkaparidontidae; Yalkaparidontia; ?Australidelphia; Marsupialia). *Journal of mammalian evolution* **21**(2), 127-172. (doi:10.1007/s10914-013-9236-3).
15. Batey I. 1907 The animal life of the Sunbury district sixty years ago. *Victorian Naturalist* **24**(4), 70-71.
16. Fleay D.H. 1935 Breeding of Dasyurus Viverrinus and General Observations on the Species. *Journal of Mammalogy* **16**(1), 10-16. (doi:10.2307/1374524).
17. Fancourt B. 2010 Spatial and temporal variation in declining eastern quoll (Dasyurus viverrinus) populations in Tasmania, University of Tasmania.
18. Altschul S.F., Gish W., Miller W., Myers E.W., Lipman D.J. 1990 Basic local alignment search tool. *Journal of Molecular Biology* **215**(3), 403-410. (doi:10.1016/S0022-2836(05)80360-2).
19. Mitchell K.J., Pratt R.C., Watson L.N., Gibb G.C., Llamas B., Kasper M., Edson J., Hopwood B., Male D., Armstrong K.N., et al. 2014 Molecular Phylogeny, Biogeography, and Habitat Preference Evolution of Marsupials. *Molecular Biology and Evolution* **31**(9), 2322-2330. (doi:10.1093/molbev/msu176).
20. Howe D. 1975 Observations on a captive marsupial mole, Notoryctes typhlops. *Australian Mammalogy* **1**(4), 361-365. (doi:10.1071/AM75007).
21. Wolf Horrell E.M., Boulanger M.C., D'Orazio J.A. 2016 Melanocortin 1 Receptor: Structure, Function, and Regulation. *Front Genet* **7**, 95. (doi:10.3389/fgene.2016.00095).

22. Consortium T.U. 2024 UniProt: the Universal Protein Knowledgebase in 2025. *Nucleic Acids Research* **53**(D1), D609-D617. (doi:10.1093/nar/gkae1010).
23. Deakin J.E. 2018 Chromosome Evolution in Marsupials. *Genes (Basel)* **9**(2), 72. (doi:10.3390/genes9020072).
24. Bond D.M., Veale A., Alexander A., Hore T.A. 2024 Coat colour in marsupials: genetic variants at the ASIP locus determine grey and black fur of the brushtail possum. *R Soc Open Sci* **11**(7), 240806. (doi:10.1098/rsos.240806).
25. Delhey K. 2019 A review of Gloger's rule, an ecogeographical rule of colour: definitions, interpretations and evidence. *Biological Reviews* **94**(4), 1294-1316. (doi:10.1111/brv.12503).
26. Lambeck K., Chappell J. 2001 Sea Level Change Through the Last Glacial Cycle. *Science* **292**(5517), 679-686. (doi:doi:10.1126/science.1059549).
27. Frankham G.J., Thompson S., Ingleby S., Soderquist T., Eldridge M.D.B. 2017 Does the 'extinct' eastern quoll *Dasyurus viverrinus* persist in Barrington Tops, New South Wales? *Australian Mammalogy* **39**(2), 243-247. (doi:10.1071/AM16029).
28. Rayner J.G., Sturiale S.L., Bailey N.W. 2022 The persistence and evolutionary consequences of vestigial behaviours. *Biological reviews of the Cambridge Philosophical Society* **97**(4), 1389-1407. (doi:10.1111/brv.12847).
29. Urban L., Santure A.W., Uddstrom L., Digby A., Vercoe D., Eason D., Crane J., Wylie M.J., Davis T., LeLec M.F., et al. 2024 The genetic basis of the kākāpō structural color polymorphism suggests balancing selection by an extinct apex predator. *PLoS Biol* **22**(9), e3002755. (doi:10.1371/journal.pbio.3002755).
30. Stammnitz M.R., Gori K., Kwon Y.M., Harry E., Martin F.J., Billis K., Cheng Y., Baez-Ortega A., Chow W., Comte S., et al. 2023 The evolution of two transmissible cancers in Tasmanian devils. *Science* **380**(6642), 283-293. (doi:doi:10.1126/science.abq6453).
31. Xiao N., Li H., Shafique L., Zhao S., Su X., Zhang Y., Cui K., Liu Q., Shi D. 2019 A Novel Pale-Yellow Coat Color of Rabbits Generated via MC1R Mutation With CRISPR/Cas9 System. *Front Genet* **10**, 875. (doi:10.3389/fgene.2019.00875).
32. Liu Z., Wen H., Hailer F., Dong F., Yang Z., Liu T., Han L., Shi F., Hu Y., Zhou J. 2019 Pseudogenization of Mc1r gene associated with transcriptional changes related to melanogenesis explains leucistic phenotypes in Oreonectes cavefish (Cypriniformes, Nemacheilidae). *Journal of Zoological Systematics and Evolutionary Research* **57**(4), 900-909. (doi:10.1111/jzs.12286).
33. Caro T. 2005 The Adaptive Significance of Coloration in Mammals. *BioScience* **55**(2), 125-136. (doi:10.1641/0006-3568(2005)055[0125:Tasoci]2.0.Co;2).
34. Cheng H., Jarvis E.D., Fedrigo O., Koepfli K.-P., Urban L., Gemmell N.J., Li H. 2022 Haplotype-resolved assembly of diploid genomes without parental data. *Nature biotechnology* **40**(9), 1332-1335. (doi:10.1038/s41587-022-01261-x).
35. Putnam N.H., O'Connell B.L., Stites J.C., Rice B.J., Blanchette M., Calef R., Troll C.J., Fields A., Hartley P.D., Sugnet C.W., et al. 2016 Chromosome-scale shotgun assembly using an in vitro method for long-range linkage. *Genome Res* **26**(3), 342-350. (doi:10.1101/gr.193474.115).
36. Manni M., Berkeley M.R., Seppey M., Simão F.A., Zdobnov E.M. 2021 BUSCO Update: Novel and Streamlined Workflows along with Broader and Deeper Phylogenetic Coverage for Scoring of Eukaryotic, Prokaryotic, and Viral Genomes. *Molecular Biology and Evolution* **38**(10), 4647-4654. (doi:10.1093/molbev/msab199).
37. Bushnell B. 2014 BBMap: a fast, accurate, splice-aware aligner. (Lawrence Berkeley National Lab.(LBNL), Berkeley, CA (United States).
38. Tian R., Han K., Geng Y., Yang C., Shi C., Thomas P.B., Pearce C., Moffatt K., Ma S., Xu S., et al. 2022 A chromosome-level genome of Antechinus flavipes provides a reference for an Australian marsupial genus with male death after mating. *Molecular ecology resources* **22**(2), 740-754. (doi:10.1111/1755-0998.13501).

39. Brandies P.A., Tang S., Johnson R.S.P., Hogg C.J., Belov K. 2020 The first Antechinus reference genome provides a resource for investigating the genetic basis of semelparity and age-related neuropathologies. *Gigabyte* **2020**, 0. (doi:10.46471/gigabyte.7).
40. Ibeh N., Feigin C.Y., Frankenberg S.R., McCarthy D.J., Pask A.J., Gallego Romero I. 2024 De novo transcriptome assembly and genome annotation of the fat-tailed dunnart (Sminthopsis crassicaudata). *GigaByte* **2024**, gigabyte118. (doi:10.46471/gigabyte.118).
41. Hogg C.J., Edwards R.J., Farquharson K.A., Silver L.W., Brandies P., Peel E., Escalona M., Jaya F.R., Thavornkanlapachai R., Batley K., et al. 2024 Extant and extinct bilby genomes combined with Indigenous knowledge improve conservation of a unique Australian marsupial. *Nature ecology & evolution* **8**(7), 1311-1326. (doi:10.1038/s41559-024-02436-2).
42. Feigin C., Frankenberg S., Pask A. 2022 A Chromosome-Scale Hybrid Genome Assembly of the Extinct Tasmanian Tiger (Thylacinus cynocephalus). *Genome Biology and Evolution* **14**(4). (doi:10.1093/gbe/evac048).
43. Dudchenko O., Batra S.S., Omer A.D., Nyquist S.K., Hoeger M., Durand N.C., Shamim M.S., Machol I., Lander E.S., Aiden A.P., et al. 2017 De novo assembly of the Aedes aegypti genome using Hi-C yields chromosome-length scaffolds. *Science* **356**(6333), 92-95. (doi:10.1126/science.aal3327).
44. Shumate A., Salzberg S.L. 2021 Liftoff: accurate mapping of gene annotations. *Bioinformatics* **37**(12), 1639-1643. (doi:10.1093/bioinformatics/btaa1016).
45. Pertea G., Pertea M. 2020 GFF Utilities: GffRead and GffCompare [version 1; peer review: 3 approved]. *F1000Research* **9**(304). (doi:10.12688/f1000research.23297.1).
46. Katoh K., Misawa K., Kuma K.-i., Miyata T. 2002 MAFFT: a novel method for rapid multiple sequence alignment based on fast Fourier transform. *Nucleic Acids Research* **30**(14), 3059-3066.
47. Zhou L., Feng T., Xu S., Gao F., Lam T.T., Wang Q., Wu T., Huang H., Zhan L., Li L., et al. 2022 ggmsa: a visual exploration tool for multiple sequence alignment and associated data. *Briefings in bioinformatics* **23**(4). (doi:10.1093/bib/bbac222).
48. Porubsky D., Guitart X., Yoo D., Dishuck P.C., Harvey W.T., Eichler E.E. 2024 SVbyEye: A visual tool to characterize structural variation among whole-genome assemblies. *bioRxiv*. (doi:10.1101/2024.09.11.612418).
49. Li H. 2018 Minimap2: pairwise alignment for nucleotide sequences. *Bioinformatics* **34**(18), 3094-3100. (doi:10.1093/bioinformatics/bty191).
50. Chen S., Zhou Y., Chen Y., Gu J. 2018 fastp: an ultra-fast all-in-one FASTQ preprocessor. *Bioinformatics* **34**(17), i884-i890. (doi:10.1093/bioinformatics/bty560).
51. Li H., Handsaker B., Wysoker A., Fennell T., Ruan J., Homer N., Marth G., Abecasis G., Durbin R. 2009 The Sequence Alignment/Map format and SAMtools. *Bioinformatics* **25**(16), 2078-2079. (doi:10.1093/bioinformatics/btp352).
52. Ramírez F., Dündar F., Diehl S., Grüning B.A., Manke T. 2014 deepTools: a flexible platform for exploring deep-sequencing data. *Nucleic Acids Res* **42**(Web Server issue), W187-191. (doi:10.1093/nar/gku365).
53. Hahne F., Ivanek R. 2016 Visualizing Genomic Data Using Gviz and Bioconductor. *Methods Mol Biol* **1418**, 335-351. (doi:10.1007/978-1-4939-3578-9_16).